Reprinted from "International Radiotherapy Review", Vol. 1, based on "The Philips 1995 International Radiotherapy Users' Meeting", Ed. R.F. Mould, pp. 21-32, 1995.

Irradiation of Target Volumes with Concave Outlines

W. De Neve, L. Fortan, S. Derycke, B. Van Duyse, and C. De Wagter

Department of Radiotherapy and Nuclear Medicine,

University Hospital, De Pintelaan 185, 9000 Gent, Belgium

Introduction

For target volumes with convex shapes, it is often not difficult to find beam incidences that isolate the target volumes from the tissues at risk. Using these beam incidences a dose distribution that conforms to the 3D shape of the target (sometimes called a 3D conformal dose distribution) can generally be obtained by dose optimisation involving human trial and error. When the target volume has concavities, it may be impossible to find beam incidences for which the target volume is isolated from the tissues at risk.

In these situations, beam intensity modulation may be required to obtain a 3D conformal dose distribution. The determination of the beam intensity profiles by human trial and error is very time consuming but practical solutions to this problem have been described by several authors and often involve a solution of the *inverse problem*.

Within this *inverse problem*, a given target volume is considered to represent the prescribed dose distribution. Several investigators have described methods to compute the beam intensity profiles (Brahme 1988), simulated annealing (Webb 1991), back projection (Bortfeld *et al* 1990). All of these methods involve the use of dedicated planning systems and none of them is easily portable to other institutions.

We are investigating a heuristic planning procedure that allows us to obtain a 3D conformal dose distribution for target volumes with concavities. This procedure divides the planning problem into a number of sub-problems each solvable by known methods. By patching together the solutions to the sub-problems a solution with a predictable dosimetric outcome can be obtained. Our procedure can be applied on most 3D planning systems and the aim of this chapter is to describe this procedure and its application in the irradiation of the macular degenerations.

1 Methods & Materials

1.1 Macular Degeneration

Macular degeneration is a vascular disease of the retina and a common cause of progressive blindness in the elderly. Treatment of subfoveal macular degeneration by laser photocoagulation (Study Group 1991), results in severe visual impairment.

It has recently been shown that radiotherapy can stop and even reverse this degenerative process (Chakravarthy *et al* 1993). Although the optimal dose is unknown, fractionated radiotherapy to total doses of 10 to 20 Gy was shown to be efficient.

These doses are above tolerance of the lens so that shielding of the lens is required. Such shielding limits the dose to the anterior parts of the retina. For these reasons irradiation is used in the treatment of subfoveal (posteriorly located) macular degenerations while laser coagulation is the treatment of choice for more anteriorly located disease.

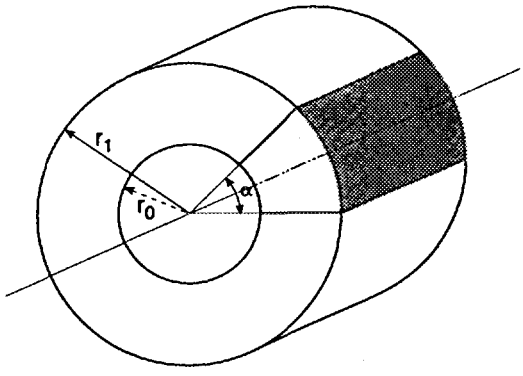

Figure 1. *Drawing of a cylindrical shell. The darkened region of this cylindrical shell is called a cylindrical shell section. r_0 is called the internal radius.*

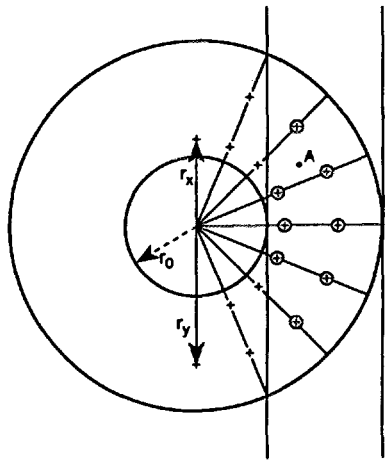

Figure 2 (above right). *Analogy of arc therapy with therapy using many static fields. In arc therapy, the dose delivered to points at distance r_x or r_y from the centre of rotation is proportional to their arc of rotation through the "ideal" beam* ***(see Appendix).*** *Assuming, instead of arc therapy, the use of a large number of equally weighted beams placed at equi-angular steps, then the dose delivered to points at distance r_x or r_y from the centre of rotation is proportional to the number of times that these points are hit by the beam (frequency of exposure). This frequency of exposure is in turn proportional to the arc of rotation through the beam. The same reasoning can be followed for beam segments. The frequency of exposure to a beam segment using static beams is proportional to the arc of rotation through the beam segment in rotation therapy. Therefore the field segmentation and segment intensities calculated for rotation therapy can also be applied with many static fields. Decreasing the number of beam incidences will decrease the analogy with rotation therapy and thus the efficacy of the gradient filters to homogenise the dose distribution.*

Using beam intensity modulation, a dose distribution was obtained that allows us to use radiotherapy irrespective of the location or extent of the disease without exceeding the tolerance of the lens. The intensity profiles of the means were computed using a heuristic method applicable to other problems involving 3D concave targets.

1.2 Planning Procedure Philosophy

The aim of our method is to reduce the planning to a problem with a known solution, namely, the deposition by arc therapy of a homogeneous dose distribution with the shape of a cylindrical shell. This reduction process is carried out in sequential steps and it is obvious that a homogeneous dose distribution, shaped as a part of a cylindrical shell (section), can be created in incomplete rotation.

Finally, the arc therapy is emulated by multiple static fields and the desired dose distribution is obtained by patching units shaped as cylindrical shell sections. Such a cylindrical shell section is drawn in **Figure 1**. Targets with a single concave region can be irradiated by stacking such cylindrical shell sections.

A dose distribution with the shape of a cylindrical shell section can be irradiated homogeneously and with distinctive edges and Brahme *et al* (1982) described an analytical solution using arc therapy. The beam intensity profile to obtain such dose distributions assumed an idealised beam profile (no divergence, no dose gradients, no penumbra).

We used a step function to approximate the intensity profiles required to homogeneously irradiate a cylindrical shell-shaped dose distribution. The nature of this step function is described in the **Appendix.** Extensions of this step function are used to irradiate a section, and allow its use with less ideal beam profiles: divergent beams and depth dose gradients.

Using arc therapy homogeneous dose distributions can be obtained by means of a beam fluence profile defined by this step-function. However, a cylindrical shell-shaped target with a centrally located cylindrically shaped tissue at risk is rarely encountered. Most deviations from this ideal situation would require continuous adaptations of the basic fluence profile to adjust for arc dependent variation in missing tissue, radiological path length and beam's-eye-view projections of target and tissue at risk.

Such continuous modulation of the beam's fluence profile is presently only feasible with the system described by Carol (1993), since beam shaping and dose intensity modulation would have to change continuously while the gantry and/or couch are rotating; with the present state of technology, such treatment, as well as its quality control, is hardly possible with conventional equipment.

It is clear that arc therapy can be emulated by a treatment with many static fields separated by equal angles. In this case, **Figure 2** shows that the basic fluence profile of the static fields is identical to that of the beam used for arc therapy.

Let us consider a point A at a distance r from the axis of rotation. Using arc therapy, the point A travels at constant angular speed through the beam while it jumps with constant angular separation through each beam segment. Using arc therapy, the dose accumulated in point A is proportional to the magnitude of the arc that it describes through each beam segment.

Using static fields separated by equal angles, the dose accumulated in point A is proportional to the number of times that it resides in each beam segment and this is again proportional to the arc spanned by each beam segment. Therefore, the basic fluence profiles for static and arc therapy are similar.

1.3 Heuristic Procedure for Planning

The planning procedure is modular and the goal of this modular process is to obtain the basic fluence profile in planes through the axis of rotation and orthogonal to the axes of the different beams. Initially, flat profiles of equal fluence are created for all beams. By adding the gradient filter, the basic fluence profile is obtained for all beams. The optimal procedure is as follows, **[1] to [6].**

[1] An axis of rotation was chosen. Although any axis of rotation can be used, we try to use an axis in the X, Y or Z direction of the treatment room. In this way, the transition from one field to the next can be performed with rotation around a single axis.

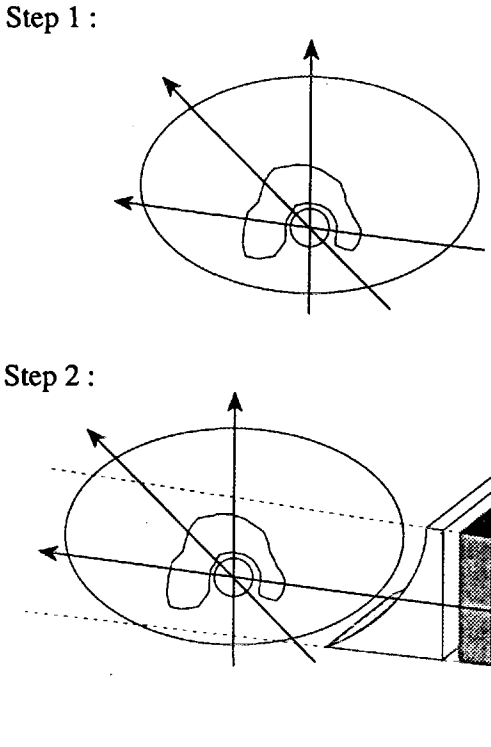

Figure 3. Horseshoe-shaped target surrounding tissue at risk. Step 1 ***(top)*** *The common isocentre of the equi-angularly separated beams is at the geometrical centre of grarity of the tissue at risk. Step 2* ***(bottom)*** *Computation of missing tissue compensation and determination of the geometry of the open beam.*

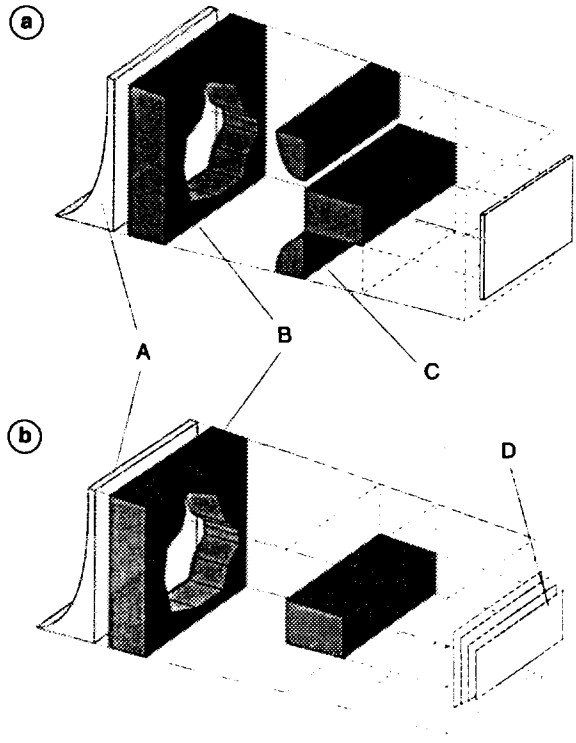

Figure 4. ***(top)*** *Blocking radiation to the tissue at risk and adding gradient filtering (C) to missing tissue compensation (A) and beam's-eye-view conformation (B).* ***(bottom)*** *Emulation of the physical gradient filter by field segmentation (D).*

A rotation of the gantry is required if the X or Y direction is used, and an isocentric rotation of the couch for the Z axis. This axis of rotation is generally located at the centre of the target's concavity, (**Figure 3** step 1).

[2] A number of equi-angularly separated beam incidences were chosen, (**Figure 3** step 1).

[3] Missing tissue was calculated in the plane described by the axes of the beams and was compensated using standard wedges or other devices, (**Figure 3** step 2). The aim of this compensation is to obtain a flat dose profile at the target.

[4] Angle dependent differences in radiological path length were calculated at the axes of the beams. By adjusting the beam weights, the contributions of (open) beams to their point of intersection were equalised. The aim is to equalise the fluence rates between all beams.

[5] Adding gradient filtering is the last step. The physical gradient filter (**Figure 4 top**) can be emulated by field segmentation (**Figure 4 bottom**). With the latter procedure, the basic fluence profile is obtained by replacing the open beams by a number of beam segments. The relative intensities of the first segments are identical to the relative intensities of the open beams.

[6] In the irradiation of macular degeneration, rotational symmetry of the beam incidences could not be obtained and the dose gradient vectors were eliminated by wedges. A two-by-two field dose gradient vector annihilation was made. In these cases, the gradient filters were added to a distorted fluence profile.

1.4 Planning System

Virtual simulation and planning was performed using the GRATIS system developed by Sherouse *et al* (1989).

2 Results & Discussion

2.1 Application to Macular Degeneration

The aim of the planning was to irradiate the largest possible fraction of retina, while at the same time to limit the dose to the lens below tolerance. Six co-planar beams in the sagittal plane (with respect to the patient) were used. Gantry positions were 0°, 30°, 60°, 90°, 120° and 330° and the couch isocentre rotation was 90°.

All beams had their isocentre at the centre of gravity of the lens. For each incidence, two field segments were used. The width of the internal segment was proportional to the radius of the protected region. In this case, it can be shown that a flat fluence profile across this segment will homogenise dose at the edge between the first and the second segment.

The computation of the relative intensity of the second to the first segment is described in the **Appendix.** A dose-volume histogram of the lens is shown in **Figure 5**. The dose distributions in a transverse and a sagittal plane through the geometric centre of the lens are shown in **Figure 6**.

3 General Applications & Conclusions

A heuristic model has been developed and was investigated to obtain 3D concave dose distributions. Its range of application is more general than the treatment of macular degeneration.

It was found applicable to the irradiation of ethmoid carcinoma and vertebral metastases in the vicinity of previously irradiated spinal cord: two cases have been treated. It is now under investigation for the irradiation of targets with more than one concavity such as cervical carcinoma and prostatic carcinoma.

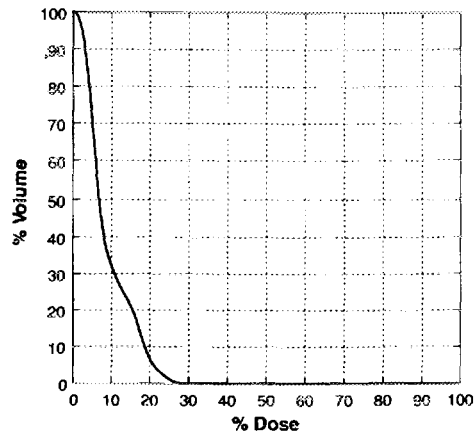

Figure 5. *Dose-volume histogram of the lens.*

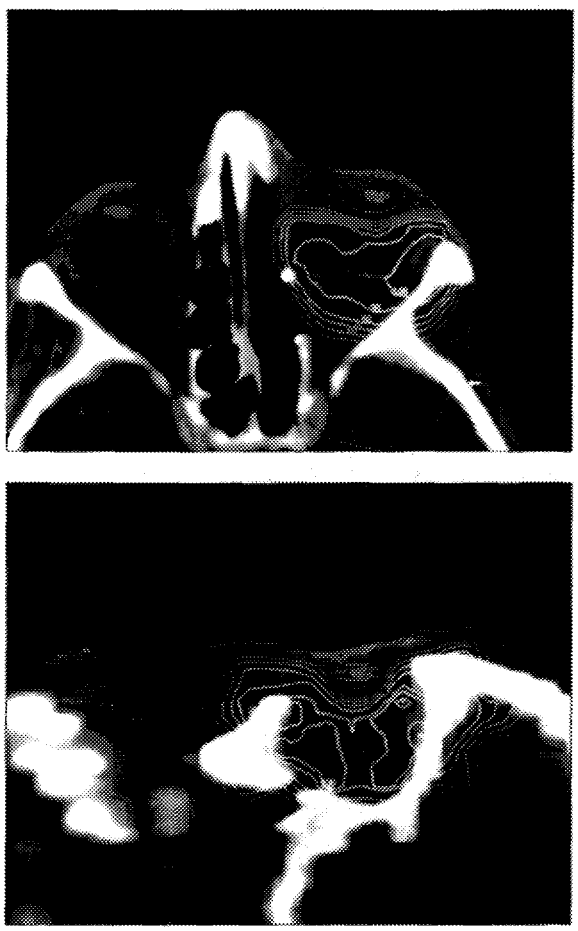

Figure 6. *Dose distributions in the transverse* ***(top)*** *and sagittal* ***(bottom)*** *planes.*

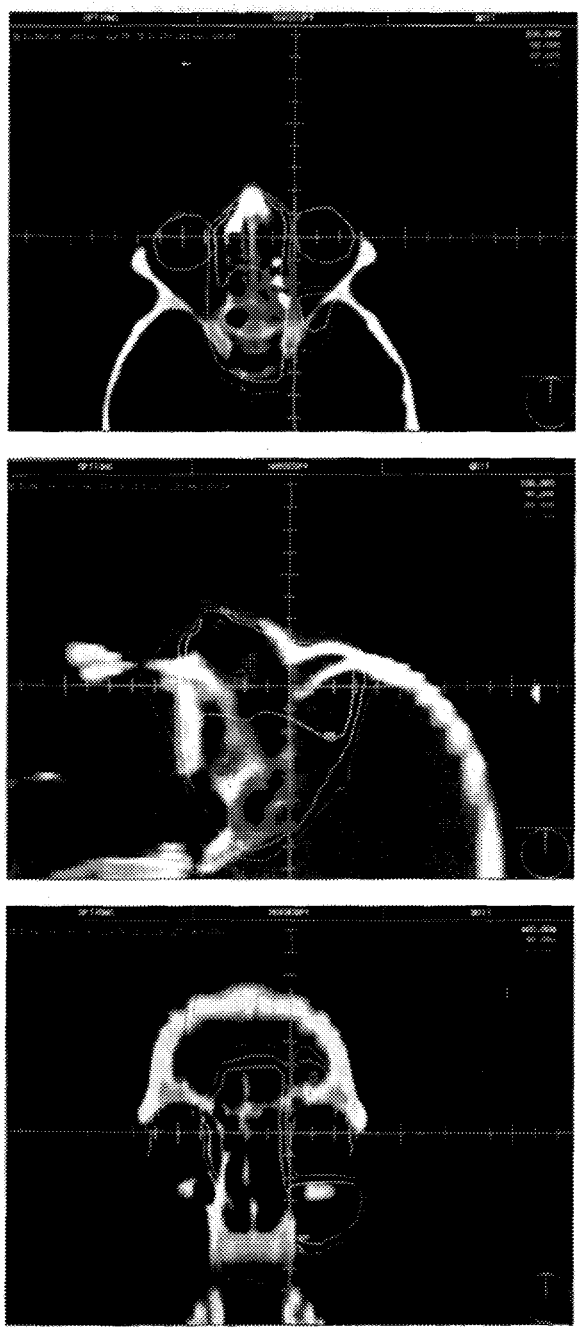

Figure 7. *Transverse, sagittal and coronal view of a dose distribution for ethmoid carcinoma with invasion of orbit, maxillary and frontal sinus.*

Appendix

1 Homogeneous Irradiation of a Cylindrical Shell

The attempt is to achieve a homogeneous irradiation of a structure with the shape of a cylindrical shell. The dose should be minimal over a radius r_0 around the axis of the cylinder and homogeneous over the thickness r_1-r_0 of the shell, **Figure 1**.

1.1 Assumptions Regarding the Beam

Non-divergent
No dose gradient
No penumbra
No scatter

1.2 Technique

360° arc around the axis of the cylinder. Beam segments of width Δx.

1.3 Homogenising the Dose

Consider a beam segment of width Δx travelling around the axis at distance r_0 at constant speed. This beam segment will cause a dose distribution that increases centrifugally for points located at distances between r_0 and $r_0 + \Delta x$ from the axis and decreases centrifugally for points located at distances further than $r_0 + \Delta x$.

Under the conditions described above the dose delivered by the beam Δx to any point at a distance r from the axis is proportional to the time that the point is exposed to the beam and this is, in turn, proportional to the angle d over which the point is irradiated by the beam Δx. Therefore the dose at any point at a distance r larger than r_0 but smaller than or equal to $r_0 + \Delta x$ from the axis is given by

$$D = c_1 . \operatorname{acos} \left(\frac{r_0}{r}\right)$$

where c_1 is a constant, representing the dose rate (and thus the beam intensity) of the first beam segment while the dose at any point at a distance larger than $r_0 + \Delta x$ is given by

$$D = c_1 . \left(\operatorname{acos} \left(\frac{r_0}{r}\right) - \operatorname{acos} \left(\frac{r_0 + \Delta x}{r}\right)\right)$$

The aim is to homogenise the cylindrical zone outside the circumference $r_0 + \Delta x$. Therefore additional beam segments of the same width Δx are added, each beam segment abutting with the previous. The dose intensity of the second beam segment is chosen so that the dose at the distance $r_0 + 2\Delta x$ is equal to the dose at the distance $r_0 + \Delta x$. By adding the third beam segment, the dose at the distance $r_0 + 3Dx$ is equalised with the doses at distances $r_0 + \Delta x$ and $r_0 + 2\Delta x$. By adding further beam segments, the dose is homogenised over the entire thickness of the cylindrical shell.

1.4 Computation of the Dose Intensity of the Second Beam Segment

The dose D_1 and the distance $r_0 + \Delta x$ is generated only by the first beam segment and is given by

$$D_1 = c_1.\text{acos}\left(\frac{r_0}{r_0 + \Delta x}\right) \qquad [1]$$

The dose D_2 at the distance $r_0 + 2\Delta x$ results from a contribution from the first and second beam segments. The contribution D_{2a} from the first beam segment is

$$D_{2a} = c_1.\left(\text{acos}\left(\frac{r_0}{r_0+2\Delta x}\right) - \text{acos}\left(\frac{r_0 + \Delta x}{r_0+2\Delta x}\right)\right) \qquad [2]$$

The contribution D_{2b} from the second beam segment is

$$D_{2b} = c_2.\left(\text{acos}\left(\frac{r_0+\Delta x}{r_0+2\Delta x}\right)\right) \qquad [3]$$

To meet the dose homogeneity requirements

$$D_1 = D_{2a} + D_{2b} \qquad [4]$$

From equations **[1]** to **[4]**, the relative dose intensities of the second and the first beam segments (c_2/c_1) can be computed

$$\frac{c_2}{c_1} = \frac{\text{acos}\left(\frac{r_0}{r_0 + \Delta x}\right) - \text{acos}\left(\frac{r_0}{r_0 + 2\Delta x}\right) + \text{acos}\left(\frac{r_0 + \Delta x}{r_0 + 2\Delta x}\right)}{\text{acos}\left(\frac{r_0 + \Delta x}{r_0 + 2\Delta x}\right)}$$

1.5 Generalisation: Relative Dose Intensity of the Beam Segment

Define $F_{n.1}$ as the relative dose intensity of the n^{th} beam segment with regard to the first beam segment.

$$F_{n.1} = \frac{c_n}{c_1}$$

By definition $F_{1.1} = 1.F_{0.1}$, and the relative dose intensity of the shielded region to the first segment is 0.

Define two terms $A_{i.n}$ and $B_{i.n}$ where

$$A_{i.n} = \text{acos}\left(\frac{r_0 + (i-1)\Delta x}{r_0 + n\Delta x}\right)$$

and

$$B_{i.n} = \text{acos}\left(\frac{r_0 + i\Delta x}{r_0 + n\Delta x}\right)$$

Now, the dose at distance $r_0 + n\Delta x$ results from the contribution of n beam segments and can be tabulated as follows.

Beam segment	Dose contributed at distance $r_0 + n\Delta x$	Remark
1	$c_1 (A_{1,n} - B_{1,n})$	$F_{1,1} = 1$
2	$c_2(A_{2,n} - B_{2,n})$	$c_2 = c_1.F_{2,1}$
3	$c_3(A_{3,n} - B_{3,n})$	$c_3 = c_1.F_{3,1}$
↓	↓	↓
n	$c_n(A_{n,n})$	$B_{n,n} = 0$

The sum of the doses contributed by the different segments can be written as follows:

$$c_1 \cdot \sum_{i=0}^{i=n-1} (F_{i,1} \cdot (A_{i,n} - B_{i,n})) + c_n.A_{n,n} \qquad [5]$$

and for dose homogeneity, this sum is equal to $c_1 A_{1,1}$ [6], the dose at distance $r_0 + Dx$.

From equations [5] and [6] we can calculate $F_{n,1}$

$$F_{n,1} = \frac{A_{1,1} - \sum_{i=0}^{i=n-1} (F_{i,1}.(A_{i,n} - B_{i,n}))}{A_{n,n}}$$

2 The Homogeneous Irradiation of a Sector of a Cylindrical Shell

Assume that we want to irradiate homogeneously a part of a cylindrical shell and consider the arc of the cylindrical shell to be α degrees (α-sector), the internal radius being r_0 and the thickness being $r_1 - r_0$ (**Figure 1**). The total arc therapy angle ϕ required to irradiate an α-sector is given by

$$\phi = \alpha + 2.\text{acos}\left(\frac{r_0}{r_1}\right)$$

Note that this solution results in a generous irradiation of structures at both sides of the α-sector.

Decreasing the internal radius of rotation at the radial edges sharpens the dose fall-off at the radial edges of an α-sector. The penalty is irradiation inside the r_0 radius and induction of more dose inhomogeneity inside the α-sector.

2.1 Beam Divergence & Dose Gradients

Divergence and dose gradients have been included in the model and are the subject of another publication. In extreme cases the dose cannot be homogenised. In clinically relevant situations, the segment intensities computed with or without taking divergence and dose gradients into account are very similar.

References

Bortfeld T., Buerkelbach J., Boesecke R. & Schlegel W., *Methods of Image Reconstruction from Projections Applied to Conformation Radiotherapy,* Physics in Medicine & Biology, **35,** 1423-1434, 1990.

Brahme A., Roos J. E. & Lax I., *Solution of an Integral Equation Encountered in Rotation Therapy*, Physics in Medicine Biology, **27**, 1221-1229, 1982.

Brahme A., *Optimisation of Stationary & Moving Beam Radiation Therapy Techniques,* Radiotherapy & Oncology, **12,** 129-140, 1988.

Carol M. P., *Integrated 3D Conformal Planning/Multivane Intensity Modulating Delivery System for Radiotherapy,* in *Proceedings of the 3D Radiation Treatment Planning & Conformal Therapy Symposium,* **Session 6,** Washington University, St. Louis, 1993.

Chakravarthy U., Houston R. F. & Archer D. B., *Treatment of Age-Related Subfoveal Neovascular Membranes by Teletherapy*, Brit. J. Opthalmology, **77**, 265-273, 1993.

Sherouse G. W., Thorn J., Novins K., Margolese-Malin L. & Mosher C., *A Portable 3D Radiotherapy Treatment Design System,* Medical Physics, **16**, 466, 1989.

Study Group on Macular Photocoagulation, *Laser Photocoagulation of Subfoveal Neovascular Lesions in Age-Related Macular Degeneration,* Archives Opthalmology, **109,** 1220-1231, 1991.

Webb S., *Optimisation by Simulated Annealing of 3D Conformal Treatment Planning for Radiation Fields Defined by a Multileaf Collimator,* Physics in Medicine & Biology, **36,** 1201-1226, 1991.